



Identifying sensitive areas of soil landscape evolution by digital soil mapping and complexity analysis in an agro-pastoral transitional zone

Shuran Gao¹, Zhuodong Zhang^{1*}, W. Marijn van der Meij², Yuxin Feng¹, Min Wu¹, Yihua Song¹

5 ¹State Key Laboratory of Earth Surface Processes and Disaster Risk Reduction, MOE Engineering Research Center of Desertification and Blown-sand Control, Faculty of Geographical Science, Beijing Normal University, Xijiekouwai Str. 19, 100875, Beijing, China

²Institute of Geography, University of Cologne, Albertus-Magnus-Platz, 50923, Cologne, Germany

*Correspondence to: Zhuodong Zhang (zzhang@bnu.edu.cn)

10 **Abstract.** Soils exhibit various development trends due to differences in initial conditions and external driving forces, leading to spatial and temporal variation in their properties. This study integrates digital soil mapping (DSM) with a modified evolutionary pathway approach (Δ complexity) to quantify horizontal and vertical soil heterogeneity across an agro-pastoral transitional zone (APTZ) in northern China. We focused on particle size distribution (PSD) and magnetic susceptibility (MS), and quantified Δ complexity between different soil depths to provide valuable insights into soil-
15 landscape evolution. This study measured the PSD and MS of 1317 samples and determined Δ complexity for 148 catchments in the study area. The R^2 for the prediction accuracy of DSM ranged between 0.481 and 0.729. The Δ complexity of PSD spans from -0.089 to 0.042 % cm^{-1} for both deep and shallow layers, whereas that of MS ranges from -0.6 to 0.96 10^{-8} $\text{m}^3 \text{kg}^{-1} \text{cm}^{-1}$. Vertical heterogeneity, which is determined by the positive and negative shifts in Δ complexity in every 5cm soil, is primarily associated with soil forming factors such as parent material, topography and vegetation, and it is further
20 regulated by tree throw and human activities. For horizontal heterogeneity, which derived from pedogenesis and also soil redistribution induced by both water and wind erosion, is determined by the positive and negative variations in both shallow and deep complexity. Our approach enables the identification of highly heterogeneous areas that may be particularly sensitive to soil change and degradation. It offers a transferable framework for assessing soil development and guiding sustainable land use. The soil Δ complexity metric provides a promising tool for analyzing and visualizing the state and
25 trends of soil-landscape evolution, and provides a scientific basis for informing land management decisions.



1 Introduction

Soil is a four-dimensional natural body (Schlichting, 1986), whose properties are variable in space and time due to differences in the soil forming factors (Jenny, 1941). Soil development follows different trajectories due to various initial conditions and external driving forces (Raab et al., 2012; Montagne et al., 2013). By acquiring abundant soil data over different spatial and temporal scales, the evolution status and trend of the soil landscapes can be inferred from the soil heterogeneity (Schlichting, 1995; Phillips, 2019). Soil mapping and its interpretation are essential for understanding the development of the soil landscape.

In recent decades, digital soil mapping (DSM) has become an important approach to develop reliable soil maps (Minasny and McBratney, 2016) that provide distinct information of soil heterogeneity for revealing soil variation and development (Kebonye et al., 2022; Rossiter et al., 2022). Soils are not isolated in the nature, but are related to their surroundings. Studies considering the spatial pattern and connections of groups of soils are therefore needed to investigate the soil development from a more comprehensive perspective.

Studies on soil heterogeneity can cover different scales. Temme et al. (2015) sampled soils from similar landscape positions of varying ages to assess how the factor time affected soil properties and their variation, which mainly focused the pedon scale. Phillips (2016) used the soil spatial adjacency graphs to represent the geography of soil landscape as a network on a landscape scale, which could be analyzed by algebraic graph theory. While such approaches capture spatial patterns, Van der Meij (2022) analyzed spatial and temporal variability outputs of a soil-landscape model to identify evolutionary pathways, which are trajectories of the temporal development of a soil landscape. This method of evolutionary pathways requires information of the spatial variation of soil properties at different stages in time, which were provided by a soil-landscape evolution model (Van der Meij et al., 2020). However, the temporal information is not easy to obtain, as there is often no information on the past states of soils and their properties. Nevertheless, the spatial patterns of soils can also reveal quantitative insights in soil heterogeneity from a new perspective. With appropriate adjustments, the evolutionary pathway method can be used to identify soil spatial heterogeneity at multiple depths, and then to determine both horizontal and vertical soil heterogeneity.

Understanding of soil heterogeneity is especially helpful in regions with significant soil variation, where this variation influences soil landscape and ecosystem development. An example of such a heterogeneous region is the widely distributed agro-pastoral transitional zone (APTZ) in North China. The soils of this zone are shaped under the joint influence of natural conditions such as geology, topography, and human factors such as cultivation, grazing and tourism. As a fragile ecological zone sensitive to environmental changes, the APTZ requires thorough understanding of soil heterogeneity to support sustainable land management and ecological conservation (Su et al., 2018; Ding et al., 2020).

In this study, digital soil mapping and a modified approach of the evolutionary pathways of Van der Meij (2022) were applied to quantify soil variation within the APTZ. The aims of the study are to (1) determine the lateral and vertical

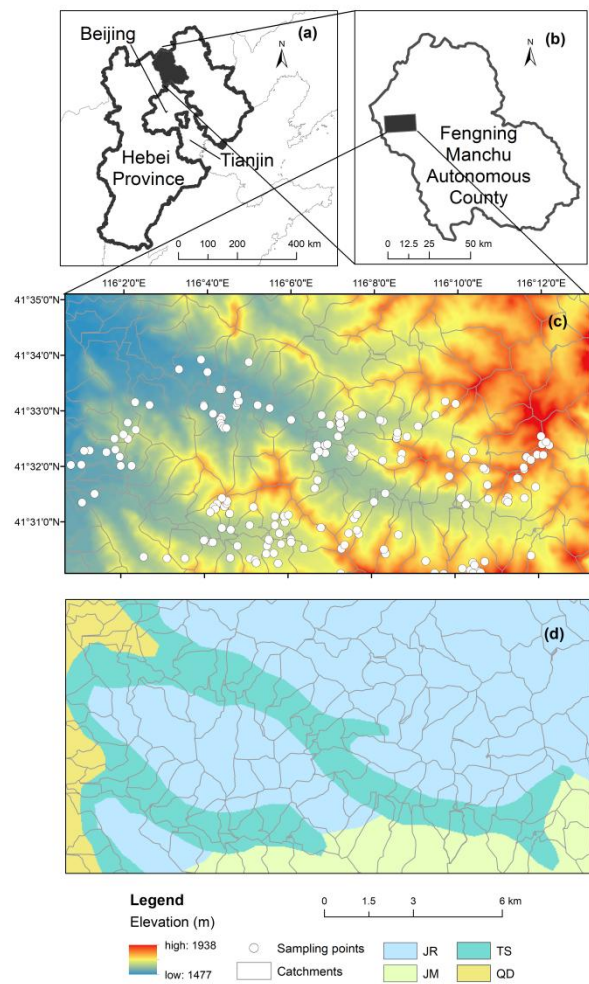


60 variations in soil properties; (2) identify the sensitive areas of landscape evolution process; (3) unravel the dominant factors and mechanisms of landscape evolution.

2 Materials and methods

2.1 Study area

The study area (116.010° E ~ 116.220° E, 41.500° N ~ 41.585° N) is located in Fengning Manchu Autonomous County, Chengde City, Hebei Province, China, with an area of 165.564 km² and an altitude of 1477—1938 m. Its topography is
65 mainly low hills and its climate type is continental monsoon climate. The current vegetation in the study area is mainly perennial herbs, and the land use type is agro-pastoral transitional zone composed of grassland, woodland and cultivated land. The parent material consists of quaternary lake alluvial deposits (QD), tertiary lake sediments (TS), Jurassic rhyolite (with andesite underlying) (JR), and late Jurassic quartz monzonite-porphyr (JM) (Chinese Geological Survey, 2015). APTZ is an
70 ecological barrier to curb desertification, and desertification moves eastward and southward. The Bashang region is a typical representative of APTZ in northern China, which is of great significance to the improvement of agricultural production and ecological environment, and plays an important strategic role in China's economic and social development and ecological environmental protection.



75 **Fig. 1** (a) Location of Hebei Province of China; (b) Location of the study area in Fengning Manchu Autonomous County; (c) Digital elevation model and sampling locations; (d) Geological map of the research area. *Note: TS = tertiary lake sediment, QD = quaternary lake alluvial deposit, JR = Jurassic rhyolite (with andesite underlying) and JM= late Jurassic quartz monzonite-porphyry.

2.2 Field sampling

80 A stratified random sampling scheme was applied, with strata based on altitude (divided into three levels by using natural split point method) and land use types (cultivated land, woodland, grassland and sparse grassland). This resulted in 15 land units. The sampling ratio and number were determined based on the proportion of each land unit within the total study area. Samples were collected in 2018. The location of the sample in the field was recorded by portable GPS. During the sampling process, an Eijkelkamp auger with a diameter of 3 cm and a length of 100 cm was used to take soil samples with 5 cm



85 increments over a depth of 40 cm, giving a total of 8 samples. Ultimately, 179 locations were sampled and 1317 samples were taken.

2.3 Laboratory measurements

Clay is an important soil property that is closely related to pedogenesis and soil strength (Cohen et al., 2010; Kurbanova et al., 2023), and it has been widely recognized as a good indicator for studying pedogenesis and soil landscape development (Shepard et al., 2017; Sadeghi et al., 2018; Zou et al., 2021). Magnetic susceptibility (MS), as a sensitive index, can effectively reflect changes in parent material, climate, topography, and drainage conditions, making it a valuable tool for assessing environmental changes (Blundell et al., 2009; Geiss et al., 2014; Ramos et al., 2017; Grison et al., 2021). Clay and χ_{lf} are both physical properties of soil that are related to pedogenesis. The combination of them can provide valuable information for exploring the soil and landscape development.

95 Soil particle size distribution of the samples was determined using the laser particle sizer method. First, the soil samples which had been sieved through 2 mm were pretreated to remove the organic matter and dispersed by adding sodium hexametaphosphate solution. Next, a MasterSizer 3000 laser particle sizer from Malvern was used to determine the particle size distribution of the pre-treated soil samples, which was repeated three times for each soil sample and averaged. Soil particle grading in this study was based on the American system (sand particles 2-0.05 mm, silt particles 0.05-0.002 mm, 100 clay particles <0.002 mm). Before the experimental analysis of soil magnetic susceptibility, all soil samples were cleaned from plant roots and stones. After the soil samples were naturally air-dried under dry and dark conditions, they passed through a plastic screen with a 2 mm aperture to filter out coarse particles. The screened soil samples were packaged in cubic plastic sample boxes with a volume of 8 cm³, respectively. Each sample was not compacted and then weighed. The volume magnetic susceptibility was measured using Bartington magnetic susceptibility meter MS2B sensor, at low frequency (0.47 105 kHz; klf) and high frequency (4.7 kHz; khf). The low-frequency mass-specific magnetic susceptibility (χ_{lf} , 10⁻⁸ m³ kg⁻¹) and frequency magnetic susceptibility (χ_{fd} , dimensionless) were calculated from the measurements by the following equations:

$$\chi_{lf} = \frac{klf \times \text{Calibration quality}}{\text{Sample quality}}, \quad (1)$$

$$\chi_{hf} = \frac{khf \times \text{Calibration quality}}{\text{Sample quality}}, \quad (2)$$

$$\chi_{fd} = \frac{\chi_{lf} - \chi_{hf}}{\chi_{lf}} \times 100\%, \quad (3)$$

110 Where χ_{lf} and χ_{hf} are the low frequency and high frequency mass-specific magnetic susceptibility of the soil sample, and calibration quality is 10 g, sample quality is the measured sample quality.



2.4 Digital soil mapping

For the digital soil mapping, a Quantile Regression Forest (QRF) from the R 4.3.0 and “quantregForest” package in RStudio
115 was used to interpolate clay content and χ_{lf} . QRF is an improved method of conventional Random Forests. 11 environmental
covariates were selected around three major soil forming factors (Table 1). Given the relatively small size of the study area,
it is assumed that the climate is uniform across the region. However, any topographical microclimate variations can be
reflected by topographic covariates, caused by topographical and other conditions can be reflected through other
environmental factors such as altitude and aspect. The parent material information of the research area was extracted from
120 the geological map of Fengning County. Topographic factors have an impact on soil formation in numerous ways. In this
research, eight topographic variables were selected. The elevation data was derived from a 30-meter resolution Digital
Elevation Model (DEM). The topographic derivatives were calculated from the DEM using ArcGIS 10.2. The analysis of
vegetation conditions encompasses two key variables, namely land use type and Normalized Difference Vegetation Index
(NDVI). The land use type is obtained through supervised classification of US Landsat imagery, while the NDVI is derived
125 from multispectral computation (reference?).

QRF can not only calculate the conditional mean of the predicted variables, but also record the complete conditional
distribution information of the predicted variables, which can be used to calculate a confidence interval. We used these
confidence intervals to calculate an Uncertainty Index (UI, Meinshausen, 2006):

$$UI = \frac{qp_{0.9} - qp_{0.1}}{qp_{0.5}}, \quad (4)$$

130 Where $qp_{0.1}$, $qp_{0.5}$ and $qp_{0.9}$ represent the predicted 10th, 50th and 90th quantile. The larger the uncertainty index, the greater the
degree of uncertainty in the predictions.



Table 1 Environmental covariates used in the quantile regression forest models.

Soil forming factor	Variable	Abbreviation	Scale/Resolution	Source
Parent material	Parent material	PM	1:50000	Chinese Geological Survey (2015)
Topography	Elevation	Ele	30 m	NASA Digital Elevation Model
	Slope aspect	Asp	30 m	
	Slope gradient	Slope	30 m	
	Curvature	Cur	30 m	
	Plan curvature	Plancur	30 m	
	Profile curvature	Profcur	30 m	
	Wetness index	WI	30 m	
Organisms	Topographic positions	TP	30 m	United States Geological Survey (Landsat 8)
	Land use	LU	30 m	
	Normalized difference vegetation index	NDVI	30 m	

2.5 Determination of soil complexity

135 Soil complexity describes the level of spatial variation or heterogeneity of soil and terrain attributes (Phillips, 2017), and is a function of soil-forming factors, nonlinear soil-forming process, internal feedbacks of the soil-landscape system and human interference (Van der Meij, 2022). The complexity of a soil landscape was defined as the spatial standard deviation of a certain soil characteristic x at a certain depth. Van der Meij (2022) used temporal changes in soil complexity to quantify whether the soil landscape showed convergent or divergent development. We modified this approach by applying the

140 method to layers from different depths rather than to different time steps; the difference between layers became Δ complexity, effectively converting the index from one of temporal heterogeneity to one of vertical spatial heterogeneity. Positive values indicate the convergent change in soil properties (the deeper layer is more homogeneous than the shallower layer), while negative values indicate a divergent change in soil properties (the deeper layer is more heterogeneous than the shallower layer). The calculation formula is as follows:

$$145 \Delta complexity_{x,d} = \frac{sd(x)_d - sd(x)_{d+\Delta d}}{\Delta d} \times 100\%, \quad (5)$$

The Δ complexity of soil was calculated for clay content and χ_{lf} data for the surface (0–5 cm), middle (20–25 cm), middle (25–30 cm) and bottom (35–40 cm) layers across the study area for soil horizontal heterogeneity analysis. Simultaneously,



the Δ complexity of the study area for clay content (with an interval of 5 cm and a total of 8 layers) was calculated layer by layer for vertical heterogeneity analysis.

150 2.6 Identification of sensitive and highly sensitive areas

The magnitude of Δ complexity is an indication for the sensitivity of an area to soil change. We applied the calculation of Δ complexity for the clay content of different layers for 148 catchments in the study area to identify sensitive catchments. Under environmental change, soils face the risk of erosion and other degradation processes. The heterogeneity of soils can be an indicator how soil properties will change under erosion. Sensitive areas are identified by the horizontal heterogeneity, 155 when the Δ complexity undergoes a positive-negative shift between deep and shallow layers. On this basis, three sensitive areas were identified by comprehensively considering the subsurface underlying surface conditions. It indicates that the soil properties in this region have been strongly influenced by environmental changes. Highly sensitive area is identified by the vertical heterogeneity. The catchment exhibiting the most frequent positive-negative shifts in Δ complexity throughout the 8-layer profile is designated as the highly sensitive area. A severe vertical heterogeneity changes will indicate a large change in 160 soil properties..

3 Results

3.1 Mapping results and reliability

3.1.1 Mapping results prediction accuracy and uncertainty evaluation

We assessed the quality of the QRF predictions using a validation dataset, resulting in the evaluation metrics reported in 165 Table 2. Quantile regression forest has good performance in predicting clay, with R^2 values ranging between 0.510 and 0.692. The low RMSE values, ranging between 1.284 to 2.782, indicate a low prediction error. The predictions of soil magnetic properties shows generally higher R^2 -values (0.547-0.729), while also producing relatively low RMSE-values (9.446-16.002, Table 2). The precision performance of the model is different when predicting soil magnetic susceptibility at different depths. We evaluated the uncertainty of QRF model prediction using UI. A higher UI indicates a wider confidence interval and a 170 higher prediction uncertainty. For the predicted clay content, the UI is highest in the surface soil layer, and generally decreases with depth (Figure 2a-d). In terms of spatial distribution, the UI of clay particles is higher in the low-altitude flood plain and river terrace areas in the northwest. Similar to clay content, the surface uncertainty of MS is relatively high (Figure 2e-h). However, the UI for lower altitude regions, such as the floodplains, increases with depth, while the other areas show a reducing UI with depth.



175 **Table 2 Accuracy evaluation of Clay and χ_{lf} prediction results.**

Depth	R ²	RMSE	R ²	RMSE
	Clay		χ_{lf}	
0-5 cm	0.692	1.284	0.729	9.446
5-10 cm	0.573	1.439	0.617	11.448
10-15 cm	0.531	1.770	0.635	14.305
15-20 cm	0.510	2.535	0.642	12.153
20-25 cm	0.533	2.368	0.547	16.002
25-30 cm	0.481	2.311	0.558	12.847
30-35 cm	0.527	2.782	0.696	11.439
35-40 cm	0.696	1.721	0.655	12.383

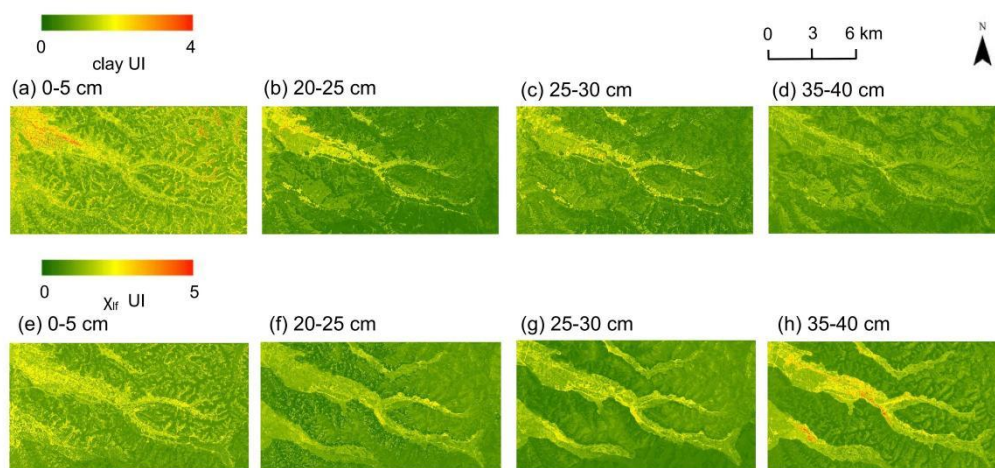


Fig. 2 Spatial distribution of UI in predictions of soil particle size distribution (a-d) and soil magnetic susceptibility (e-h) for different soil depths.

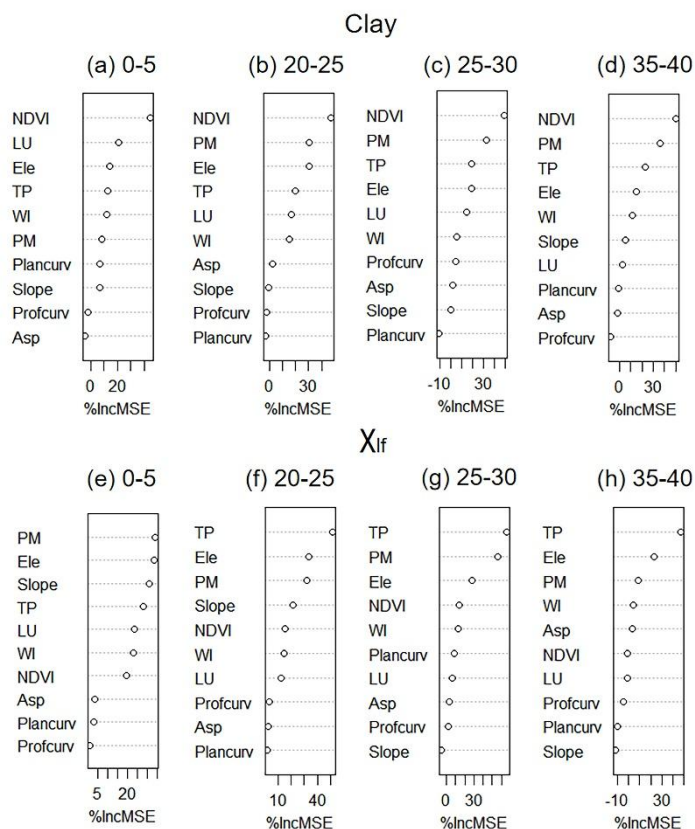
180 **3.1.2 Importance of environmental covariates**

Fig. 3 shows the relative importance of the different environmental covariates for the QRF predictions. For the clay content (Fig. 3a-d), the NDVI is the most important predictor. The second is parent material, which ranks second in the ranking of clay for multiple depths. Other important environmental covariates for clay content prediction are topography, elevation and land use..

185 Fig. 3(e-h) shows the relative importance of the predictions for χ_{lf} . The ranking of environmental predictor importance varies with soil depth. For χ_{lf} , the most important environmental covariant is topographic position (TP), which ranks first among the



three layers except the surface layer 0-5 cm, while parent material (PM) ranks first in the surface layer. The second most important ones are elevation and parent material, which are mostly in the second and third place.



190 **Fig. 3** Relative importance of environmental covariates in predicting clay and χ_{lf} using the Quantile Regression Forest.

3.1.3 Predicted maps of clay and χ_{lf}

Fig. 4(a-d) shows the prediction results of each layer of clay content in the study area. The spatial distribution of clay content changes significantly, and it shows a gradual trend of increasing from layer to layer. Generally speaking, the clay content in different depths shows similar spatial distribution characteristics. In the fork-shaped zone in the northwest of the study area, the soil is characterized by low content of clay as low as 3%, while in the south and east, the clay content gradually increases from the surface to the bottom, and the soil texture is finer.

Fig. 4(e-h) shows the same spatial patterns as texture for soil magnetic susceptibility, with low values in the river area (as low as $11 \cdot 10^{-8} \text{ m}^3 \text{ kg}^{-1}$), while higher altitudes generally show higher values for magnetic susceptibility (up to $140 \cdot 10^{-8} \text{ m}^3 \text{ kg}^{-1}$, which is 12 times higher than the low value areas).

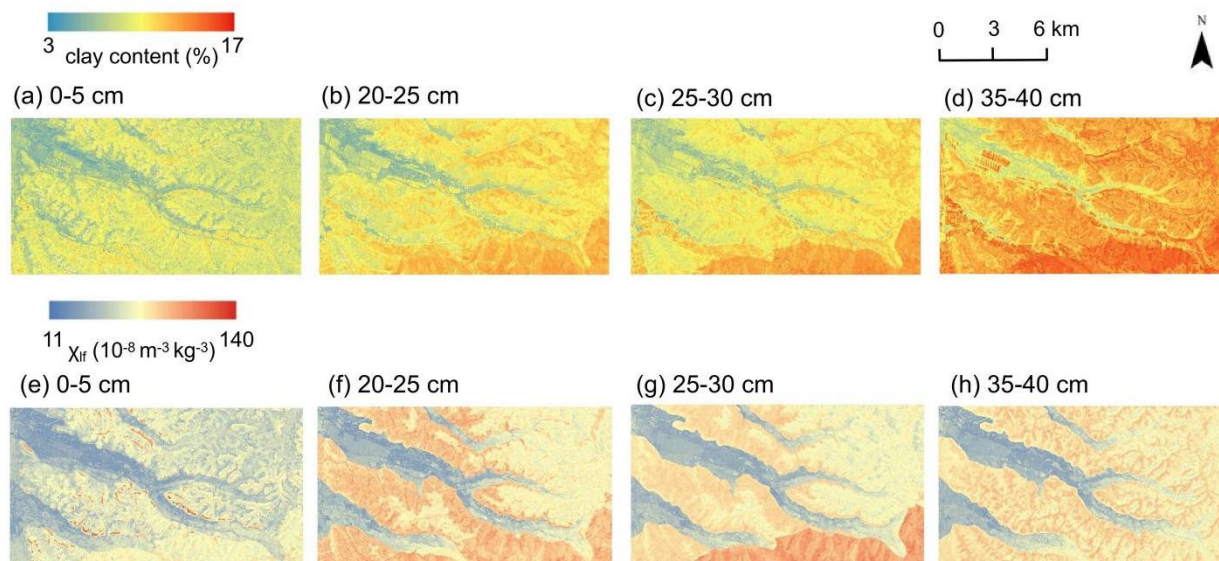


Fig. 4 Mapping results of clay content (a-d) and χ_{lf} (e-h) for different depths.

3.2 Soil complexity analysis

205 Fig. 5 (a-b) shows the soil Δ complexity calculated according to the catchment area by using the predicted data of soil clay
 content in the study area. The soil Δ complexity was calculated for 0-25 cm (a, 0-5 cm and 20-25 cm, two layers) and 25-40
 cm (b, 25-30 cm and 35-40 cm, two layers). By calculating the Δ complexity of soil properties in different depth, the
 sensitive areas with large changes in soil properties in the study area can be identified. In Fig. 5 (a-b) the Δ complexity index
 of the catchments near the rivers and river terraces in the northwest and central regions is generally negative in both deep and
 210 shallow layers, indicating divergent soil properties with depth. The Δ complexity index of catchment in the eastern high
 altitude area was negative in the deep layers, that is, divergent transform, but it becomes positive in the shallow layers, and
 tends to be convergent transform. The blue areas in Fig. 5 (a) show convergent transform. Compared with the Δ complexity
 index in Fig. 5 (b), these catchments are divergent in the deep layers, which suggests that these regions tend to be more
 responsive to environmental change. Combined with the soil Δ complexity calculated based on low-frequency magnetic
 215 susceptibility in Fig. 5 (c-d), it is more certain that the three areas with red boxes in the study area are indeed sensitive areas.

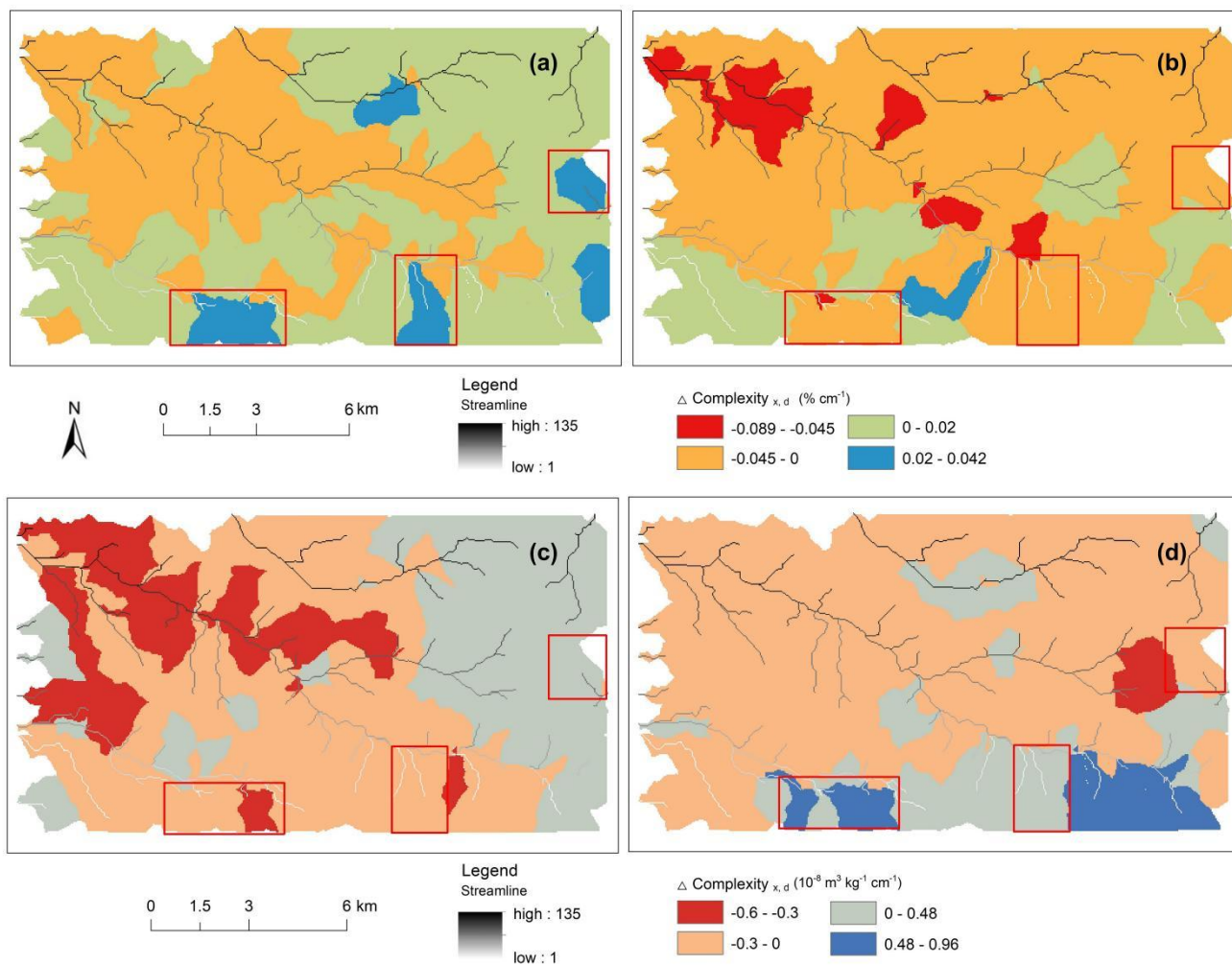


Fig. 5 The spatial heterogeneity of soil Δ complexity in (a) shallow layers, (b) deep layers based on clay content calculation (within the red boxes are the determined sensitive areas). The spatial heterogeneity of soil Δ complexity in (c) shallow layers, (d) deep layers based on χ_{lf} calculation (within the red box are the determined sensitive areas).

220

3.3 Spatial heterogeneity of clay Δ complexity under different conditions

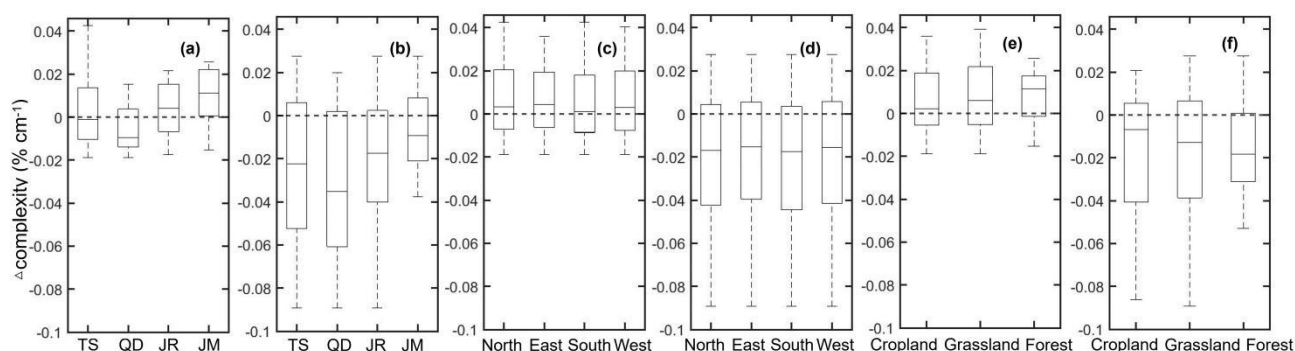
The parent material will determine the change of soil particle size distribution, and also affect the Δ complexity of soil. As shown in Fig. 6 (a-b), on the TS (tertiary lake sediment) and QD (quaternary lake alluvial deposit) parent materials, the soil Δ complexity in the deep and shallow layers is mostly negative, indicating divergent transform. On JR and JM, the soil



225 Δ complexity is negative in the deep layers, that is, divergent transform, and positive in the shallow layers, which becomes convergent transform. Among them, the change of soil Δ complexity on JM is the most obvious.

In Fig. 6 (c), most of the changes in soil Δ complexity on each slope of the study area were positive, while most of the changes in In Fig. 6 (d) were negative. Different from the characteristics of soil Δ complexity change of parent material and land use type, the changes of soil Δ complexity are almost identical in the same layer. Across virtually all slope aspects, the shallow layers evolved in convergence while the deep layers evolved in divergence.

230 In Fig. 6 (e-f) that clay contents are most affected in forest. In shallow layers, the Δ complexity of forest is mostly positive, indicating convergent transformation, while in deep layers it is negative, indicating divergent transformation. Cropland and grassland also have similar patterns, but not as obvious as forest.



235

Fig. 6 Box plots of Δ complexity in clay content under different environmental conditions and for different depths. Δ complexity for different parent materials for (a) shallow layers, and (b) deep layers. *Note: TS = tertiary lake sediment, QD = quaternary lake alluvial deposit, JR = Jurassic rhyolite (with andesite underlying) and JM= late Jurassic quartz monzonite-porphry. Δ complexity for different slope aspects for (c) shallow layers, and (d) deep layers. Δ complexity for different land use types for (e) shallow layers, and (f) deep layers.

240

3.4 Complexity vertical heterogeneity of typical catchments and identification of highly sensitive area

The external influencing factors are different in different regions of the study area, so different catchments may follow different development trajectories. To illustrate this, we calculated Δ complexity for nine typical catchments from three different locations in the study area (Figure 7). We increased the vertical resolution of Δ complexity by reducing the depth intervals for the calculations. Figure 8 shows the depth profiles of Δ complexity in these typical catchments. As can be seen from the bottom to the top in Fig. 8 (a), the lowland catchments show that in the deep layer, these three watersheds first evolved in a divergent way, then changed into convergent transform at 20-30 cm, and then changed into divergent transform

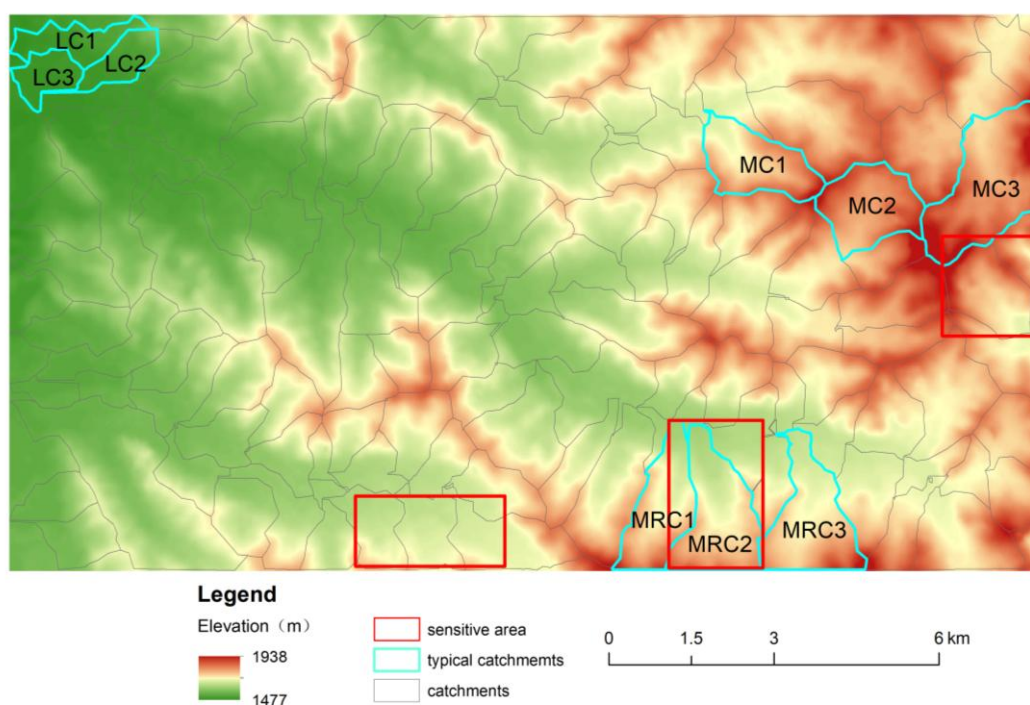
245



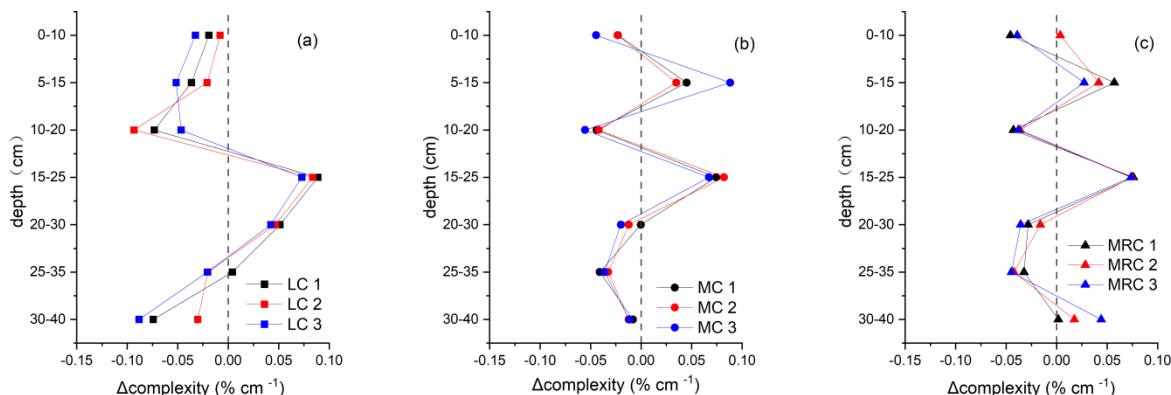
250 after 10-20 cm. Mountainous catchments (Figure 8b) and mixed-relief catchments (Figure 8c) show other development tracks, with alternating convergent and divergent transform.

Section 3.2 and this section are show the results of soil Δ complexity calculated at different depth intervals. Considering the two results together, the highly sensitive area with stronger response to environmental changes are identified. The area where the red and blue boxes overlap in Fig. 7 is the final identified highly sensitive area - MRC 2. Zone C is a highly sensitive area because its soil complexity shows significant variations across different layers.

255



260 **Fig. 7 Spatial distribution of typical catchments: lowland catchments: LC 1-3 (Lowland Catchment 1-3); mountainous catchments: MC 1-3 (Mountainous Catchment 1-3); mixed-relief catchments: MRC 1-3 (Mixed-Relief Catchment 1-3) and sensitive areas based on soil Δ complexity.**



265 **Fig. 8 Soil Δ complexity depth profiles for clay content in three typical catchments from (a) LC 1-3 (Lowland Catchment 1-3), (b) MC 1-3 (Mountainous Catchment 1-3), and (c) MRC 1-3 (Mixed-Relief Catchment 1-3).**

4 Discussion

4.1 Advantages of Δ complexity method to DSM

270 DSM aims to accurately depict soil spatial distribution but lacks of quantification of soil properties. While the Δ complexity has the advantage in quantifying the variation characteristics of soil properties across vertical and horizontal scales. Some researchers have studied soil landscape heterogeneity through statistical analysis of obtained soil properties (Temme et al., 2015; Nimalka Sanjeevani et al., 2024), but the lack of spatial visualization limits the interpretation of their geographic distribution and the association between regions.

275 In order to explore the development process of soil landscape, a stride from the pedon scale to the soil continuum within the landscape is needed (Sommer et al., 2008). The DSM approach mainly predicts area soil properties. However, previous research on DSM mostly focused on mapping (Wang et al., 2024; Cheng et al., 2024), lacking spatial connections between the grids, and conventional outputs primarily represent static spatial distributions. It lacks descriptions of the horizontal spatial distribution variability of data within a certain area, as well as the vertical spatial variations between different layers of the same region. With the advancement of 3D digital soil mapping techniques, there is an increasing capability to model 280 soil properties continuously throughout the soil profile (Malone et al., 2014; Kidd et al., 2015). Nevertheless, the inherent three-dimensionality of these datasets presents significant challenges for visualization and interpretation, because direct visualization of 3D soil data is often computationally demanding and can overwhelm end-users with excessive multiple information, hindering practical applications in land management and soil research as conventional (Sun et al., 2023). 2D maps remain the primary medium for communicating soil spatial information to researchers and stakeholders (Kokalj and



285 Somrak., 2019). Consequently, effective methods are urgently needed to condense depth-profile information into comprehensible 2D representations without losing critical information about vertical variability.

In this study, the obtained DSM was reprocessed, and the soil Δ complexity of the properties was calculated using the catchment as the unit, so as to evaluate the spatial heterogeneity of the soil in the study area. The spatial connections among DSM grids are revealed. By calculating the difference between $sd(x)_{\Delta d}$ and $sd(x)_{d+\Delta d}$ of small intervals, Δ complexity integrates the vertical variation into a single index and reveals the variation trend of soil profile heterogeneity in vertical direction, and makes up for the deficiency of DSM in describing the dynamic process (Grunwald et al., 2011). Similarly, the calculation of Δ complexity of large intervals in the catchment can reveal the horizontal heterogeneity of soil properties in the whole study area. This approach effectively bridges the gap between detailed 3D soil models and accessible 2D visualization, enabling the identification of zones with different profiles of development trends that would otherwise be obscured in traditional layer-by-layer mapping approaches. Through this method, the redistribution process of soil can be analyzed.

295 Soil complexity indicate that the development trajectory of soil varies under different environmental conditions. Pedogenesis and soil redistribution jointly sculpt highly sensitive area. By analyzing the trajectory of soil, a basis for land management in the APTZ and methods to improve the soil landscape sustainability can be provided. By synergizing the approaches, highly sensitive areas can be delineated, and the entire approach can be can be applied broadly in soil research.

300 **4.2 Drivers of vertical soil heterogeneity and pedogenic interpretation**

The soil profile is progressively imprinted by pedogenesis and can, in turn, be read to infer which specific pedogenic processes have been dominant and influential through its developmental trajectory. Three representative catchment types have been identified, and their distinct soil development trajectories have been quantified, revealing divergent pedogenic pathways.

305 The first type profile shows the parent material dominated development trajectories of lowland catchments 1-3 (LC 1-3) (Fig. 8a). The deep layers in these areas are formed by the accumulation of lake alluvium. The lake receives suspended sediments primarily from river discharge (Zhai et al., 2006). In Fig. 8(a), the Δ complexity at depths of 25 - 40 cm range from -0.1 to 0 \% cm^{-1} , indicating a divergent transform from the upper to lower layers. This suggested that new soil materials with uniform internal clay content were transported into the upper part of the 25-40 cm layer. This aligns with the view of Temme et al. (2015) that divergent transform may have been provided by raw parent material. The development trajectories of LC 1-3 exhibit a convergent transform within the 15-30 cm layer, Δ complexity range from 0.05 to 0.1 \% cm^{-1} (Fig. 8a). During this period, populations may gradually moved to utilize the soil, which leads to an uneven distribution of clay content in the upper soil across this depth range, resulting in short-term convergent transform. Another divergent transformation emerges within the 0–20 cm, with the excessive utilization of land by humans, causing surface soil homogenization (Xu et al., 2005).
315 Therefore, the evolution of this type is dominated by PM, and with additional influence of human.



The second type of profile present vegetation dominated trajectories for mountainous catchments 1-3 (MC 1-3) in Fig. 8 (b). In addition to the different mountainous topography compared to the first type of lowland, the vegetation coverage of these three catchments has also increased obviously, accompanied by a rise in tree density, which in turn leads to more frequent tree throw. Since the tree throw occurs intermittently, the development trajectories of MC 1-3 show a turning point from negative to positive between 5-15 cm and 15-25 cm. The process of tree throw disturbs the soil (Hancock et al., 2021). Although the tree throw cannot explain all sediment fluxes, it is undeniable that it has an impact on soil (Ferdowsi et al., 2018). Additionally, in the process of afforestation, operations such as excavation and landfill can also disturb the soil that causing vertical heterogeneity (Qin, 2020). It should be noted that the vertical heterogeneity of these catchments is not entirely caused by tree throw or planting trees, nor does it rule out the influence of topography.

As shown in Fig. 8 (c), the third type of profile displays topography-vegetation dominated trajectories of mixed-relief catchments 1-3 (MRC 1-3). Compared to the second type, the third type catchments exhibit greater complexity due to their larger altitude range, larger slope gradient and severer water erosion. Within these catchments, the Δ complexity range from -0.05 to 0.1 \% cm^{-1} and exhibit five sign changes from the surface to the bottom layer, corresponding to an oscillating pattern of divergence-convergence transitions. Topography, especially slope gradient, has a great influence on clay at different depths (Li, 2019; Beczek et al., 2024). In addition, the distribution of parent material (lake sediments and igneous rocks) and vegetation (forest, grassland, and cropland) in these three catchments are also different, and this difference lead to the result of soil complexity trajectory.

In summary, the analysis reveals that soil vertical heterogeneity in representative catchments arises from the foundational influences of parent material, vegetation and topography, while tree throw and human activities further modulate these patterns. The layered maps of clay content merely display point-specific, layer-by-layer numerical values, quantifying "how much" clay exists at each location. By calculating Δ complexity, however, the analysis transcends isolated point measurements to capture the spatial heterogeneity of clay distribution across the entire catchment, allowing the overall uniformity of clay distribution across the entire catchment to be characterized.

4.3 The shaping of horizontal heterogeneity pattern by soil redistribution

Pedogenesis exerts a strong influence on vertical heterogeneity, yet soil evolution is not confined to downward profile development, it also involves lateral redistribution at broader spatial scales. Fig. 5 reveals a pronounced horizontal heterogeneity. Soil redistribution is primarily driven by water and wind erosion.

The study area exhibits water erosion (Wang et al., 2020), which leads to the erosion induced redistribution of clay (Vaezi et al., 2017). In Fig. 5, Δ complexity of the two properties exhibit distinct evolutionary directions in both the deep and shallow layers across the eastern and southeastern parts of the study area. These areas are mountains with steep slopes, higher precipitation and different vegetation cover. Catchments with steeper slopes exhibit a greater potential for transporting fine particles (Vaezi et al., 2017). Therefore, clay content in the eastern region is unevenly distributed, with Δ complexity



ranging from 0 to 0.042 % cm^{-1} , indicating convergent transform in the shallow layer. The different vegetation in the eastern region can also lead to uneven distribution of clay particles in the catchment (Dodd and Quinton, 2015). For the western part of the study area, Δ complexity of the two layers ranges from -0.089 to 0 % cm^{-1} , the terrain is relatively flat and the vegetation is monotonous, so the vast majority of the area shows divergent transform.

Apart from water erosion, the study area is also a region with severe soil wind erosion. So the exogenous soil particles inputs of wind erosion must also be considered to explain the soil particles horizontal heterogeneity. Soil particles with particle size >0.84 mm are defined as not wind-eroded particles (Fryrear et al., 1994). Northwest wind carries away the soil particles on western flats and partially deposits the particles in the eastern forest. The interception effect of vegetation on sand particles is an important factor in the redistribution of surface particles (Albiach et al., 2001). There are both forest and grassland in the east, the interception effect of wind erosion is different (Sun et al., 2016; Qin, 2020), so the clay content in the east of the study area change greatly in the shallow layer, which Δ complexity is between 0 and 0.042 % cm^{-1} . Similarly, in the northwest of the study area, due to roughly identical soil forming factors, deep-layer clay content varies little across catchments, with Δ complexity ranging from -0.045 to 0 % cm^{-1} , showing divergent changes. In the shallow layer, the wind blows away the erodible particles in the region, and the soil landscape showed a divergent transform.

Overall, the vertical and horizontal heterogeneity patterns act as a high-resolution fingerprint of landscape history, they archive the relative imprint of parent material, topography, vegetation, episodic tree throw and anthropogenic disturbance in the profile, while simultaneously recording the spatial signature of wind and water driven particle redistribution across the land surface. Thus, present day soil Δ complexity can be turned into an integrated mirror of past and ongoing landscape evolution. Moreover, it can provide a 2D expression for 3D mapping that conveys multiple information.

4.4 Potential refinements for future work

By calculating the Δ complexity at different depths, areas sensitive to environmental changes can be identified. Yet different layers of soil formed at different ages. Chronosequences transform spatial differences between soils into temporal differences (Huggett, 1998; Walker et al., 2010), which are helpful for understanding the rate of soil change (Dethier et al., 2012; Temme et al., 2015). In erosive and sedimentary landscapes, soil materials are detached, transported, and deposited via natural and anthropogenic processes. Such soil acts as archives to infer landscape change stages and rates, aiding in understanding past and current landscape dynamics (Dotterweich, 2008). However, chronosequences is not employed in this study. If the samples in the study area can be built up an optically stimulated luminescence (OSL) in the future and if the evolutionary pathways can be calculated according to the Δ complexity of soil in different periods, then the understanding of the development of soil landscape will be more complete.

Currently, Δ complexity is primarily assessed based on a single soil property (such as clay or χ_{it}). In the future, it would be valuable to explore integrated Δ complexity indices that incorporate multiple soil properties simultaneously. Moreover, the



specific formation mechanisms underlying Δ complexity need to be further clarified through field investigations, such as
380 detailed soil profile descriptions.

5 Conclusions

This study measured the clay and χ_{lf} of 1317 samples from the agro-pastoral transition zone in northern China. The study used QRF to conduct digital soil mapping of soil properties, and calculates the Δ complexity of the mapping results based on catchments.

385 The Δ complexity of clay ranges from -0.089 to 0.042 % cm^{-1} , and the complexity of MS ranges from -0.6 to 0.96 $10^{-8} \text{ m}^3 \text{ kg}^{-1} \text{ cm}^{-1}$. Soil properties including clay and χ_{lf} show obvious heterogeneity in the agro-pastoral landscape. The vertical heterogeneity of soil Δ complexity of clay is affected by soil forming factors such as parent material, topography and vegetation, it is further influenced by tree throw and human activities. The vertical heterogeneity of the lowland catchments is caused by sediment accumulation and human activities. The vertical heterogeneity of the mountainous catchments is
390 caused by tree throwing and topography. The vertical heterogeneity of the mixed-relief catchments is influenced by topography and vegetation, and this kind of catchments is located in the southeast of the study area where water erosion is more serious.

The horizontal heterogeneity of clay is manifested in different development directions in the deep and shallow layers of the western and eastern parts of the study area. This is not only related to pedogenesis, but also to soil redistribution caused by
395 wind and water erosion. The transition in horizontal heterogeneity of χ_{lf} between deep and shallow layers occurs in the same regions where the clay transition is observed. The transition between deep and shallow layers with distinct characteristics is identified as the sensitive areas in this study.

Besides the commonly used DSM, this study employed the Δ complexity heterogeneity approach to explore soil landscape development, quantifying the change of soil properties, which can visualize spatial heterogeneity of soil landscape in an
400 alternative perspective and effectively identify the highly sensitive areas. Such findings are helpful for inferring the formation mechanism of soil landscape and the rational management of the APTZ.

Code and data availability

The data and code supporting the findings of this study are not publicly available but can be obtained from the corresponding author upon reasonable request.



405 **Author contributions**

Shuran Gao: sample data collection; original draft; writing and revision; Zhuodong Zhang: conceptualization; methodology; review and editing; W. Marijn van der Meij: methodology; review and editing; Yuxin Feng: review and editing; Min Wu: sample data collection; Yihua Song: sample data collection.

Competing interests

410 At least one of the (co-)authors serves as topic editor for the special issue to which this paper belongs.

Disclaimer

Publisher's note: Copernicus Publications remains neutral with regard to jurisdictional claims in published maps and institutional affiliations.

Acknowledgements

415 Special appreciation was given to Jingwen Rao, Zheng Zhou and other participants for field sampling works, to Dr. Xiaofei Gao for support of laboratory work, to Yue Du for laboratory measurement, to Yuhe Shen and Yixuan Zhou for assistance in modeling.

Financial support

This study was supported by a project funded by the National Natural Science Foundation of China (42477346), and projects
420 funded by the State Key Laboratory of Earth Surface Processes and Disaster Risk Reduction, China (2024-TS-08, 2024-ZD-02).

Review statement

The review statement will be added by Copernicus Publications listing the handling editor as well as all contributing referees according to their status anonymous or identified.

425



References

- Albiach, R., Canet, R., Pomares, F., and Ingelmo, F.: Organic matter components and aggregate stability after the application of different amendments to a horticultural soil, *Bioresource Technology*, 76, 125–129, [https://doi.org/10.1016/S0960-8524\(00\)00090-0](https://doi.org/10.1016/S0960-8524(00)00090-0), 2001.
- 430 Beczek, M., Mazur, R., Beczek, T., Ryżak, M., Sochan, A., Gibała, K., Polakowski, C., and Bieganowski, A.: The effect of slope incline on the characteristics of particles ejected during the soil splash phenomenon, *Geoderma*, 441, 116757, <https://doi.org/10.1016/j.geoderma.2023.116757>, 2024.
- Blundell, A., Dearing, J. A., Boyle, J. F., and Hannam, J. A.: Controlling factors for the spatial variability of soil magnetic susceptibility across England and Wales, *Earth-Science Reviews*, 95, 158–188, <https://doi.org/10.1016/j.earscirev.2009.05.001>, 2009.
- 435 Cheng, L., Yan, M., Zhang, W., Guan, W., Zhong, L., and Xu, J.: Interpretable Digital Soil Organic Matter Mapping Based on Geographical Gaussian Process-Generalized Additive Model (GGP-GAM), *Agriculture*, 14, 1578, <https://doi.org/10.3390/agriculture14091578>, 2024.
- Chinese Geological Survey, 2015. National 1:50,000 regional geological map. [http://](http://219.142.81.39/newgsigrid/CGSGeoData/Default.aspx?per=true)
- 440 219.142.81.39/newgsigrid/CGSGeoData/Default.aspx?per=true.
- Cohen, S., Willgoose, G., and Hancock, G.: The mARM3D spatially distributed soil evolution model: Three-dimensional model framework and analysis of hillslope and landform responses, *J. Geophys. Res.*, 115, 2009JF001536, <https://doi.org/10.1029/2009JF001536>, 2010.
- Dethier, D. P., Birkeland, P. W., and McCarthy, J. A.: Using the accumulation of CBD-extractable iron and clay content to estimate soil age on stable surfaces and nearby slopes, Front Range, Colorado, *Geomorphology*, 173–174, 17–29, <https://doi.org/10.1016/j.geomorph.2012.05.022>, 2012.
- Ding, Z., Zhang, Z., Li, Y., Zhang, L., and Zhang, K.: Characteristics of magnetic susceptibility on cropland and pastureland slopes in an area influenced by both wind and water erosion and implications for soil redistribution patterns, *Soil and Tillage Research*, 199, 104568, <https://doi.org/10.1016/j.still.2019.104568>, 2020.
- 450 Dotterweich, M.: The history of soil erosion and fluvial deposits in small catchments of central Europe: Deciphering the long-term interaction between humans and the environment — A review, *Geomorphology*, 101, 192–208, <https://doi.org/10.1016/j.geomorph.2008.05.023>, 2008.
- Emission and Reflection Radiometer Global Digital Elevation Model (ASTER GDEM) <http://www.gscloud.cn>.
- Ferdowsi, B., Ortiz, C. P., and Jerolmack, D. J.: Glassy dynamics of landscape evolution, *Proc. Natl. Acad. Sci. U.S.A.*, 115, 4827–4832, <https://doi.org/10.1073/pnas.1715250115>, 2018.
- 455 Fryrear, D. W., Krammes, C. A., Williamson, D. L., and Zobeck, T. M.: Computing the wind erodible fraction of soils, *Journal of Soil and Water Conservation*, 49, 183–188, <https://doi.org/10.1080/00224561.1994.12456849>, 1994.



- Grison, H., Petrovsky, E., and Hanzlikova, H.: Assessing anthropogenic contribution in highly magnetic forest soils developed on basalts using magnetic susceptibility and concentration of elements, *CATENA*, 206, 105480, 460 <https://doi.org/10.1016/j.catena.2021.105480>, 2021.
- Grunwald, S., Thompson, J. A., and Boettinger, J. L.: Digital Soil Mapping and Modeling at Continental Scales: Finding Solutions for Global Issues, *Soil Science Soc of Amer J*, 75, 1201–1213, <https://doi.org/10.2136/sssaj2011.0025>, 2011.
- Hancock, G. and Lowry, J.: Quantifying the influence of rainfall, vegetation and animals on soil erosion and hillslope connectivity in the monsoonal tropics of northern Australia, *Earth Surf Processes Landf*, 46, 2110–2123, 465 <https://doi.org/10.1002/esp.5147>, 2021.
- Huggett, R. J.: Soil chronosequences, soil development, and soil evolution: a critical review, *CATENA*, 32, 155–172, [https://doi.org/10.1016/S0341-8162\(98\)00053-8](https://doi.org/10.1016/S0341-8162(98)00053-8), 1998.
- Jenny, H.: Factors of soil formation: a system of quantitative pedology, *Soil Science*, 52, 415, <https://doi.org/10.1097/00010694-194111000-00009>, 1941.
- 470 Kebonye, N. M., Agyeman, P. C., Seletlo, Z., and Eze, P. N.: On exploring bivariate and trivariate maps as visualization tools for spatial associations in digital soil mapping: A focus on soil properties, *Precision Agric*, 24, 511–532, <https://doi.org/10.1007/s11119-022-09955-7>, 2023.
- Kidd, D., Malone, B., McBratney, A., Minasny, B., and Webb, M.: Operational sampling challenges to digital soil mapping in Tasmania, Australia, *Geoderma Regional*, 4, 1–10, <https://doi.org/10.1016/j.geodrs.2014.11.002>, 2015.
- 475 Kokalj, Ž. and Somrak, M.: Why Not a Single Image? Combining Visualizations to Facilitate Fieldwork and On-Screen Mapping, *Remote Sensing*, 11, 747, <https://doi.org/10.3390/rs11070747>, 2019.
- Kurbanova, F., Makeev, A., Aseyeva, E., Kust, P., Khokhlova, O., Puzanova, T., Sverchkova, A., and Kozmirchuk, I.: Pedogenic response to Holocene landscape evolution in the forest-steppe zone of the Russian Plain, *CATENA*, 220, 106675, <https://doi.org/10.1016/j.catena.2022.106675>, 2023.
- 480 Li, A.: Prediction of spatial distribution of main soil texture types in chongqing influenced by topographic factors, Ph. D, Southwest University, 108pp., 2019. (in Chinese with English abstract).
- Minasny, B. and McBratney, Alex. B.: Digital soil mapping: A brief history and some lessons, *Geoderma*, 264, 301–311, <https://doi.org/10.1016/j.geoderma.2015.07.017>, 2016.
- Montagne, D., Cousin, I., Josière, O., and Cornu, S.: Agricultural drainage-induced Albeluvisol evolution: A source of 485 deterministic chaos, *Geoderma*, 193–194, 109–116, <https://doi.org/10.1016/j.geoderma.2012.10.019>, 2013.
- Meinshausen, N. and Ridgeway, G.: Quantile Regression Forests, *Journal of Machine Learning Research*, 7(2), 983–999, 2006.
- Malone, B. P., McBratney, A. B., Minasny, B., and Laslett, G. M.: Mapping continuous depth functions of soil carbon storage and available water capacity, *Geoderma*, 154, 138–152, <https://doi.org/10.1016/j.geoderma.2009.10.007>, 2009.
- 490 National Aeronautics and Space Administration. Advanced Spaceborne Thermal Emission and Reflection Radiometer Global Digital Elevation Model (ASTER GDEM)[DB/OL]. <http://www.gscloud.cn>. 2009.



- Nimalka Sanjeevani, H. K., Samarasinghe, D. P., and De Costa, W. A. J. M.: Influence of elevation and the associated variation of climate and vegetation on selected soil properties of tropical rainforests across a wide elevational gradient, *CATENA*, 237, 107823, <https://doi.org/10.1016/j.catena.2024.107823>, 2024.
- 495 Ola, A., Dodd, I. C., and Quinton, J. N.: Can we manipulate root system architecture to control soil erosion?, *SOIL*, 1, 603–612, <https://doi.org/10.5194/soil-1-603-2015>, 2015.
- Phillips, J. D.: Identifying sources of soil landscape complexity with spatial adjacency graphs, *Geoderma*, 267, 58–64, <https://doi.org/10.1016/j.geoderma.2015.12.019>, 2016.
- Phillips, J. D.: Soil Complexity and Pedogenesis, *Soil Science*, 182, 117–127, <https://doi.org/10.1097/SS.000000000000204>, 2017.
- 500 Phillips, J. D.: Evolutionary Pathways in Soil-Geomorphic Systems, *Soil Science*, 184, 1–12, <https://doi.org/10.1097/SS.000000000000246>, 2019.
- Qin, L.: Study on the windbreak and sand fixation effects of afforestation in Bashang area, Hebei Province, Hebei Normal University, 10.27110/d.cnki.ghsfu.2020.001279, 2020. (in Chinese with English abstract).
- 505 Raab, T., Krümmelbein, J., Schneider, A., Gerwin, W., Maurer, T., and Naeth, M. A.: Initial Ecosystem Processes as Key Factors of Landscape Development—A Review, *Physical Geography*, 33, 305–343, <https://doi.org/10.2747/0272-3646.33.4.305>, 2012.
- Ramos, P. V., Dalmolin, R. S. D., Marques Júnior, J., Siqueira, D. S., Almeida, J. A. D., Moura-Bueno, J. M., Universidade Federal do Rio Grande do Sul, Brasil, Universidade Federal de Santa Maria, Brasil, Universidade Estadual Paulista, Brasil, 510 Universidade Estadual Paulista, Brasil, Universidade do Estado de Santa Catarina, Brasil, and Universidade Federal de Santa Maria, Brasil: Magnetic Susceptibility of Soil to Differentiate Soil Environments in Southern Brazil, *Rev. Bras. Ciênc. Solo*, 41, <https://doi.org/10.1590/18069657rbc20160189>, 2017.
- Rossiter, D. G., Poggio, L., Beaudette, D., and Libohova, Z.: How well does digital soil mapping represent soil geography? An investigation from the USA, *SOIL*, 8, 559–586, <https://doi.org/10.5194/soil-8-559-2022>, 2022.
- 515 Sadeghi, S. H., Gharemahmudli, S., Kheirfam, H., Khaledi Darvishan, A., Kiani Harchegani, M., Saeidi, P., Gholami, L., and Vafakhah, M.: Effects of type, level and time of sand and gravel mining on particle size distributions of suspended sediment, *International Soil and Water Conservation Research*, 6, 184–193, <https://doi.org/10.1016/j.iswcr.2018.01.005>, 2018.
- Schlichting, E.: *Introduction Into Soil Science*, 131pp, 1986.
- 520 Schlichting, E., Blume, H.-P., and Stahr, K.: *Soils Practical*, 295pp, 1995.
- Shepard, C., Schaap, M. G., Pelletier, J. D., and Rasmussen, C.: A probabilistic approach to quantifying soil physical properties via time-integrated energy and mass input, *SOIL*, 3, 67–82, <https://doi.org/10.5194/soil-3-67-2017>, 2017.
- Sommer, M., Gerke, H. H., and Deumlich, D.: Modelling soil landscape genesis — A “time split” approach for hummocky agricultural landscapes, *Geoderma*, 145, 480–493, <https://doi.org/10.1016/j.geoderma.2008.01.012>, 2008.



- 525 Su, W., Li, Z., and Chen, S.: Evolution Trend of Vegetation Coverage and Its Risk Assessment in the Bashang Region in Hebei Province, *Arid Zone Research*, 35 (03), 686–694, [10.13866/j.azr.2018.03.23](https://doi.org/10.13866/j.azr.2018.03.23), 2018. (in Chinese with English abstract).
- Sun, C., Liu, G., and Xue, S.: Land-Use Conversion Changes the Multifractal Features of Particle-Size Distribution on the Loess Plateau of China, *IJERPH*, 13, 785, <https://doi.org/10.3390/ijerph13080785>, 2016.
- Sun, J., Xie, X., Pan, Y., Islamov, Y., Ge, Y., and Yu, H.: Visualization of 3D Hyperspectral Soil Mapping Data via
530 Autoencoder-based Clustering, in: 2023 IEEE International Conference on Big Data (BigData), 2023 IEEE International Conference on Big Data (BigData), 3503–3509, <https://doi.org/10.1109/BigData59044.2023.10386924>, 2023.
- Temme, A. J. A. M., Lange, K., and Schwering, M. F. A.: Time development of soils in mountain landscapes—divergence and convergence of properties with age, *J Soils Sediments*, 15, 1373–1382, <https://doi.org/10.1007/s11368-014-0947-8>, 2015.
- United States Geological Survey. American Earth observation satellite (Landsat 8) [DB/OL]. <http://glovis.usgs.gov/>. 2017-
535 04-09.
- Vaezi, A. R., Abbasi, M., Keesstra, S., and Cerdà, A.: Assessment of soil particle erodibility and sediment trapping using check dams in small semi-arid catchments, *CATENA*, 157, 227–240, <https://doi.org/10.1016/j.catena.2017.05.021>, 2017.
- Van Der Meij, W. M.: Evolutionary pathways in soil-landscape evolution models, *SOIL*, 8, 381–389, <https://doi.org/10.5194/soil-8-381-2022>, 2022.
- 540 Van Der Meij, W. M., Temme, A. J. A. M., Wallinga, J., and Sommer, M.: Modeling soil and landscape evolution – the effect of rainfall and land-use change on soil and landscape patterns, *SOIL*, 6, 337–358, <https://doi.org/10.5194/soil-6-337-2020>, 2020.
- Walker, L. R., Wardle, D. A., Bardgett, R. D., and Clarkson, B. D.: The use of chronosequences in studies of ecological succession and soil development, *Journal of Ecology*, 98, 725–736, <https://doi.org/10.1111/j.1365-2745.2010.01664.x>, 2010.
- 545 Wang, L., Li, Z., Nie, X., Liu, Y., Wang, H., Li, Y., and Li, J.: Three-dimensional spatiotemporal variation of soil organic carbon and its influencing factors at the basin scale, *International Soil and Water Conservation Research*, 12, 885–895, <https://doi.org/10.1016/j.iswcr.2024.05.001>, 2024.
- Wang, Y., Dong, Y., and Su, Z.: Assessment of soil erosion change under land use and reforestation scenarios, *JOURNAL OF NATURAL RESOURCES*, 35, 1369, <https://doi.org/10.31497/zrzyxb.20200610>, 2020.
- 550 Wang, Y. and Li, Y.: Soil Particle size differentiation of haloxylonammოდendron sand-break forest in southern margin of gurbantunggut desert, *Bulletin of Soil and Water Conservation*, 40 (03), 75–80, [10.13961/j.cnki.stbctb.2020.03.011](https://doi.org/10.13961/j.cnki.stbctb.2020.03.011), 2020. (in Chinese with English abstract).
- Wilson, M. J.: The importance of parent material in soil classification: A review in a historical context, *CATENA*, 182, 104131, <https://doi.org/10.1016/j.catena.2019.104131>, 2019.
- 555 Xu, W., Luo, G., Chen, X., and Xiao, L.: Effects of Land Use Patterns and Intensity on the Distribution of Soil Granularity in the Oases in Arid Areas, *Arid Land Geography*, 28(6), 800–804, [10.3321/j.issn:1000-6060.2005.06.015](https://doi.org/10.3321/j.issn:1000-6060.2005.06.015), 2005. (in Chinese with English abstract).

<https://doi.org/10.5194/egusphere-2026-1837>

Preprint. Discussion started: 9 April 2026

© Author(s) 2026. CC BY 4.0 License.



- Zhai, Q., Guo, Z., Li, Y., and Li, R.: Annually laminated lake sediments and environmental changes in Bashang Plateau, North China, *Palaeogeography, Palaeoclimatology, Palaeoecology*, 241, 95–102, 560 <https://doi.org/10.1016/j.palaeo.2006.06.011>, 2006.
- Zhou, X., Zhou, Y., and Feng, Q.: Main influencing factors of soil particle distribution in the karst basin, *CATENA*, 224, 107002, <https://doi.org/10.1016/j.catena.2023.107002>, 2023.
- Zou, X., Zhang, Z., Wu, M., and Wan, Y.: Slope-scale spatial variability of fractal dimension of soil particle size distribution at multiple depths, *Soil Science Soc of Amer J*, 85, 117–131, <https://doi.org/10.1002/saj2.20178>, 2021.